



Cross Interaction Drives Stratification in Drying Film of Binary Colloidal Mixtures

Jiajia Zhou,^{1,2,*} Ying Jiang,^{1,2,†} and Masao Doi^{2,‡}

¹Key Laboratory of Bio-Inspired Smart Interfacial Science and Technology of Ministry of Education, School of Chemistry and Environment, Beihang University, Beijing 100191, China

²Center of Soft Matter Physics and Its Applications, Beihang University, Beijing 100191, China

(Received 21 December 2016; published 8 March 2017)

When a liquid film of a colloidal solution consisting of particles of different sizes is dried on a substrate, the colloids often stratify, where smaller colloids are laid upon larger colloids. This phenomenon is counterintuitive because larger colloids which have a smaller diffusion constant, are expected to remain near the surface during the drying process, leaving a layer of larger colloids on top of smaller colloids. Here we show that the phenomenon is caused by the interaction between the colloids, and can be explained by a diffusion model accounting for the interaction between the colloids. By studying the evolution equations both numerically and analytically, we derive the condition at which the stratified structures are obtained.

DOI: 10.1103/PhysRevLett.118.108002

The drying of a colloidal film is important in many areas, such as in printing [1], spreading and coating [2], and materials science [3,4]. An important problem is how the structure of dried film is controlled by drying conditions. It is known that the spatial distribution of colloidal particles in the drying process is determined by two competing processes. One is Brownian motion [5–7], which is characterized by the diffusion constant D , and the other is evaporation [4], characterized by the speed v_{ev} at which the surface recedes. The competition between them can be quantified by the film formation Peclet number $Pe = v_{ev}h_0/D$ [8], where h_0 is the initial thickness of the film. If $Pe < 1$, the concentration gradient created by evaporation is quickly flattened by diffusion, and the colloid concentration remains uniform. On the other hand, if $Pe > 1$, the concentration gradient increases, and the colloids accumulate near the top of the film.

If there are two types of colloids of different size [9–12], the above consideration predicts that the larger colloids will accumulate near the free surface (*large-on-top*), because larger colloids have a smaller diffusion constant, and therefore a larger Peclet number. Recently, however, the opposite phenomenon has been reported by Fortini and co-workers [13]. By simulation and experiments, they have shown that smaller colloids appear on top of larger colloids (*small-on-top*). They argued that this is due to the osmotic pressure of smaller colloids, but no quantitative theory has been given.

In this Letter, we show that the phenomenon can be explained by the standard diffusion model [14] if the interaction between colloids is taken into account. We will use a simple hard-sphere model, and show that the small-on-top structure is created by the cross interaction between colloids of different sizes. The effect of cross interaction on colloidal motion is not symmetric: it is much stronger on larger colloids than smaller colloids and pushes the larger colloids towards the bottom of the film. We will give a criterion for when the small-on-top structure is created as

well as the corresponding experimental conditions, such as the drying rate, initial colloidal concentrations, and size ratio.

Evolution equations.—We consider a thin film composed of two types of colloids of different sizes in solution (see Fig. 1). In a thin-film geometry, the lateral flow is not important and the film can be assumed to dry one dimensionally. The evolution of the film height is $h(t) = h_0 - v_{ev}t$, where v_{ev} is the evaporation rate. The colloids are hard spheres with the radius r_1 and r_2 (assuming $r_1 < r_2$) and their volumes are $\nu_i = 4\pi r_i^2/3$ ($i = 1, 2$). We define the size ratio by $\alpha = r_2/r_1 > 1$. The time-dependent volume fraction and number density are $\phi_i(z, t)$ and $n_i = \phi_i/\nu_i$, respectively. Initially the colloidal solution is homogeneous with the volume fractions $\phi_i(z, 0) = \phi_{0i}$.

For a dilute hard-sphere mixture, the free-energy density can be written as

$$\frac{1}{k_B T} f(\phi_1, \phi_2) = \sum_i \frac{1}{\nu_i} \phi_i \ln \phi_i + \sum_{i,j} \frac{1}{\nu_i \nu_j} a_{ij} \phi_i \phi_j, \quad (1)$$

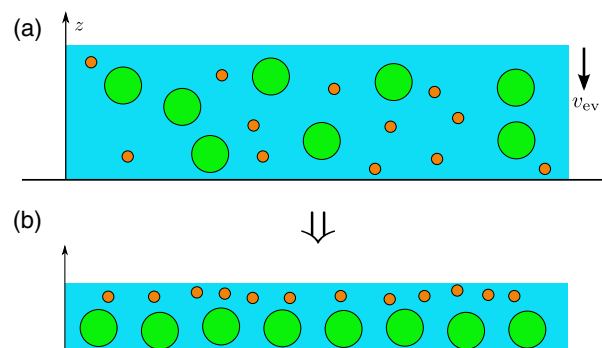


FIG. 1. Drying of a binary colloidal solution in a film makes a stratified film with small colloids on top of large colloids.

where $a_{ij} = (2\pi/3)(r_i + r_j)^3$ is the second-order virial coefficient for hard spheres. The chemical potential μ_i is then given by

$$\mu_i = \frac{\partial f}{\partial n_i} = k_B T \left(\ln \phi_i + 1 + 2 \sum_j \frac{a_{ij}}{v_j} \phi_j \right). \quad (2)$$

The average velocity $v_i(z)$ of the colloids at z is determined by the balance of two forces. One is the thermodynamic force, which is given by the gradient of the chemical potential (2). The other is the hydrodynamic drag, which is related to the colloid velocity v_i by $\zeta_i v_i$, where ζ_i is the friction constant per colloid. The balance of these forces gives the average velocity

$$v_i = -\frac{1}{\zeta_i} \frac{\partial \mu_i}{\partial z} = -\frac{D_i}{k_B T} \frac{\partial \mu_i}{\partial z}, \quad (3)$$

where we have used the Einstein relation $D_i = k_B T / \zeta_i$. In general, the diffusion constant takes a matrix form and depends on the colloidal concentrations due to direct and hydrodynamic interactions [5–7]. Here we have only kept the diagonal terms and neglected the concentration dependence.

Given the velocity v_i , the time evolution of ϕ_i is obtained by the conservation equation

$$\frac{\partial \phi_i}{\partial t} = -\frac{\partial \phi_i v_i}{\partial z}. \quad (4)$$

Equations (2)–(4) give

$$\frac{\partial \phi_i}{\partial t} = \frac{\partial}{\partial z} \left(\phi_i D_i \frac{\partial \mu_i}{\partial z} \right). \quad (5)$$

Using the relation $r_2/r_1 = \alpha$ and $\nu_2/\nu_1 = \alpha^3$, the average velocities are explicitly written as

$$v_1 = -D_1 \left[\left(\frac{1}{\phi_1} + 8 \right) \frac{\partial \phi_1}{\partial z} + \left(1 + \frac{1}{\alpha} \right)^3 \frac{\partial \phi_2}{\partial z} \right], \quad (6)$$

$$v_2 = -D_2 \left[(1 + \alpha)^3 \frac{\partial \phi_1}{\partial z} + \left(\frac{1}{\phi_2} + 8 \right) \frac{\partial \phi_2}{\partial z} \right]. \quad (7)$$

The time evolution equations are

$$\frac{\partial \phi_1}{\partial t} = D_1 \frac{\partial}{\partial z} \left[(1 + 8\phi_1) \frac{\partial \phi_1}{\partial z} + \left(1 + \frac{1}{\alpha} \right)^3 \phi_1 \frac{\partial \phi_2}{\partial z} \right], \quad (8)$$

$$\frac{\partial \phi_2}{\partial t} = D_2 \frac{\partial}{\partial z} \left[(1 + \alpha)^3 \phi_2 \frac{\partial \phi_1}{\partial z} + (1 + 8\phi_2) \frac{\partial \phi_2}{\partial z} \right]. \quad (9)$$

These are coupled diffusion equations. They can also be derived from the Onsager principle [7,15]. The boundary conditions at the substrate $z = 0$ are $v_1 = v_2 = 0$. At the free surface $z = h$, $v_1 = v_2 = -v_{ev}$.

The coupled diffusion equations (8) and (9) can be made dimensionless by scaling the length to the initial film

thickness h_0 and the time to the evaporation time scale $\tau = h_0/v_{ev}$ [15]. This procedure introduces two Peclet numbers

$$\text{Pe}_1 = \frac{v_{ev} h_0}{D_1}, \quad \text{Pe}_2 = \frac{v_{ev} h_0}{D_2} = \alpha \text{Pe}_1. \quad (10)$$

Here we have used Stokes-Einstein relation $D_i = k_B T / 6\pi\eta r_i$, where η is the fluid viscosity.

We solved the coupled diffusion equations numerically. Figure 2 shows the representative concentration profiles at various times.

When both Peclet numbers are less than 1 [Fig. 2(a)], the perturbation due to the evaporation is small, and the concentration profiles for both colloids remain almost uniform, with slightly increase near the free surface. When both Peclet numbers are greater than 1 [Fig. 2(c)], the free surface recedes faster than the diffusion, and the concentration becomes nonuniform. Initially, both colloids accumulated at the free surface, but at later times, the concentration gradient of the smaller colloid becomes large, and eventually drives the big colloids to the bottom. Figure 2(b) shows the intermediate state, where the concentration profile of large colloid near the free surface becomes flat at late times but a clear stratification has not yet fully developed.

Analytic theory.—We can understand the mechanism by taking a close look at the average velocities (6) and (7). If there is no interaction between the colloids, the equations take a simple form

$$v_i = -D_i \left(\frac{1}{\phi_i} \frac{\partial \phi_i}{\partial z} \right), \quad (11)$$

which gives a pair of uncoupled diffusion equations

$$\frac{\partial \phi_i}{\partial t} = D_i \frac{\partial^2 \phi_i}{\partial z^2}. \quad (12)$$

In Eqs. (6) and (7), the $8(\partial \phi_i / \partial z)$ terms come from the self-interaction (virial coefficient a_{ii}), while the $(1 + 1/\alpha)^3 (\partial \phi_2 / \partial z)$ and $(1 + \alpha)^3 (\partial \phi_1 / \partial z)$ terms originate from the cross interaction (virial coefficients $a_{12} = a_{21}$). One can immediately see that the cross-interaction term affects the larger colloids much more strongly than the smaller colloids due to the factor of $(1 + \alpha)^3$.

The small-on-top structure forms when the first term in Eq. (7) becomes larger than the second term, due to either a large size ratio α or a strong concentration gradient of smaller colloids $\partial \phi_1 / \partial z$. In this case, the larger colloids are driven to the substrate while the smaller colloids are left near the top surface. The condition for this phenomenon to happen can be written as

$$(1 + \alpha)^3 \frac{\partial \phi_1}{\partial z} > C \frac{1}{\phi_2} \frac{\partial \phi_2}{\partial z}, \quad (13)$$

where C is a factor which can be regarded as a fitting parameter in our model. Since our theory accounts for the

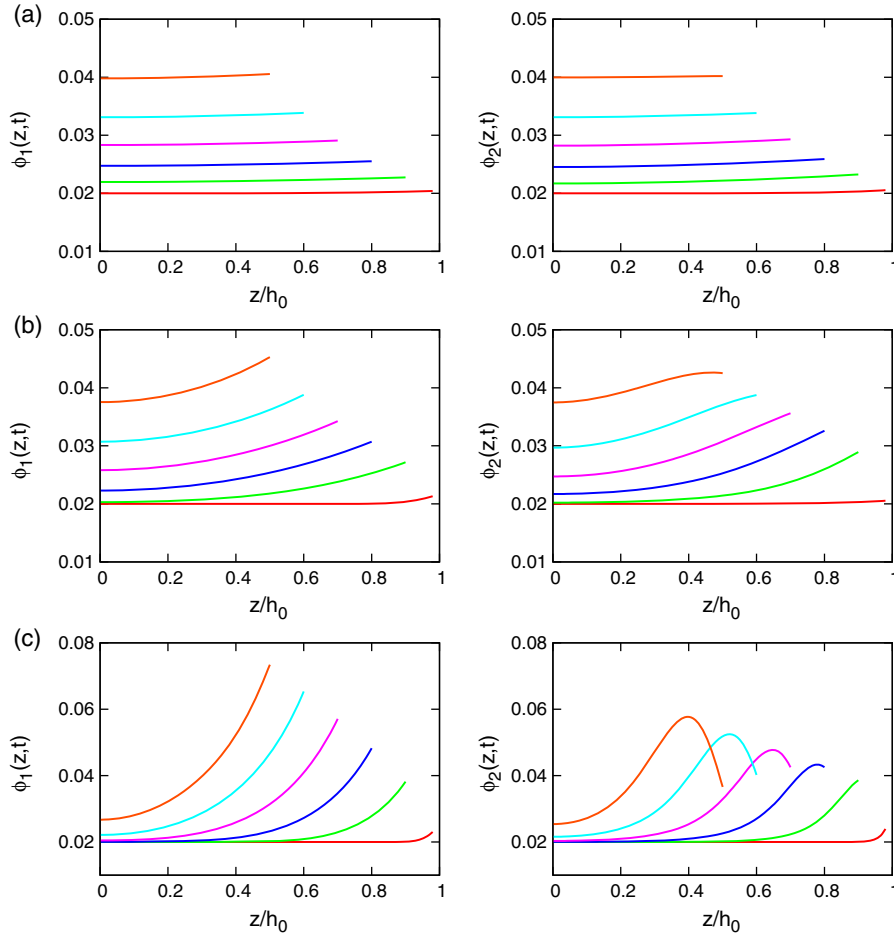


FIG. 2. Time variation of concentration profile of colloidal particles having size ratio $\alpha = 4$: (a) $Pe_1 = 0.1$, $Pe_2 = 0.4$; (b) $Pe_1 = 1$, $Pe_2 = 4$; (c) $Pe_1 = 5$, $Pe_2 = 20$. The initial concentrations are $\phi_{01} = \phi_{02} = 0.02$. The curves from bottom to top correspond to time $\tau = 0.005, 0.1, 0.2, 0.3, 0.4, 0.5$.

effect of interaction up to the second-order term, we expect the condition (13) to be valid at dilute regimes. At late times, the stratified structure formed at low concentration would persist over to higher concentrations and the final film remains small-on-top structure.

We can write the condition (13) in terms of experimental parameters. We use the results for noninteracting colloids from Eq. (11) as a first-order approximation. The evolution of a drying film with one type of colloid [14,17] or polymer [18–20] has been studied. In Ref. [19], the same diffusion model was used and analytic results are derived at the surface,

$$\frac{\partial \phi_i}{\partial z} = \frac{v_{ev}}{D_i} \phi_{hi} \quad (14)$$

$$\phi_{hi} \approx \left(1 + \sqrt{\frac{4v_{ev}^2 t^{1/2}}{\pi D_i}}\right) \phi_{0i} \approx (1 + Pe_i) \phi_{0i} \quad (15)$$

In the second equation, we have used the characteristic time $t = h_0^2/D_i$.

The condition for the small-on-top structure (13) is then simplified,

$$(1 + \alpha)^3 \frac{v_{ev}}{D_1} \phi_{h1} > C \frac{1}{\phi_2} \frac{v_{ev}}{D_2} \phi_{h2} \Rightarrow (1 + \alpha)^3 \frac{D_2}{D_1} \phi_{h1} > C. \quad (16)$$

Hence for large α , the condition is

$$\alpha^2(1 + Pe_1)\phi_{01} > C. \quad (17)$$

It is interesting to note that the condition (17) does not depend on ϕ_{02} . This is plausible because the cross-interaction term in Eq. (7), which is responsible for driving the large colloids to the bottom, does not depend on ϕ_{02} . The size ratio comes in terms of α^2 in (17), indicating that the size asymmetry has a strong effect on the stratification.

State diagrams.—To test our analytic formula, we solved the coupled diffusion equations (8) and (9) for large sets of parameters ($Pe_1, \alpha, \phi_{01}, \phi_{02}$). We stopped the numerical calculation when $h = h_0/2$ and regarded the structure at this state as the indicative of the final structure. We did this because our model ceases to be valid at high concentrations and whether or not the system takes the stratified structure can be discussed at this state.

We extrapolated the concentration profile at the last step of the calculation, and constructed an expected state

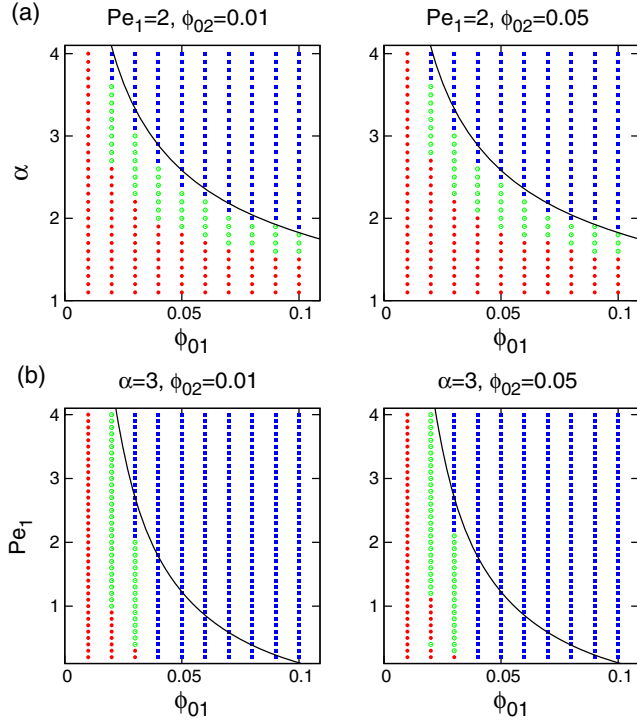


FIG. 3. (a) State diagrams in the ϕ_{01} - α plane. Parameters are $Pe_1 = 2$, $\phi_{02} = 0.01$ (left), and $\phi_{02} = 0.05$ (right). (b) State diagrams in the ϕ_{01} - Pe_1 plane. Parameters are $\alpha = 3$, $\phi_{02} = 0.01$ (left), and $\phi_{02} = 0.05$ (right). The solid curve corresponds to $\alpha^2(1+Pe_1)\phi_{01} = 1$.

diagram of the dried state. We judged the dried state will have the small-on-top structure if there is a peak of ϕ_2 , i.e., if $\partial\phi_2/\partial z|_{z=h}$ is negative at the last step of the calculation. We used blue squares (filled squares) to indicate these states. If $\partial\phi_2/\partial z|_{z=h}$ is positive, and for some value of z in the range of $0 < z < h$, $\phi_2(z)$ has a negative curvature (i.e., $\partial^2\phi_2/\partial z^2 < 0$), the small-on-top structure may form at late times. Therefore we classified the state as intermediate (open circle). Otherwise, the dried state will have either the large-on-top structure or almost homogeneous distributions of both smaller and larger colloids. We labeled these states using the symbol (filled circle). These states are shown in Fig. 3.

Figure 3(a) shows the results in the ϕ_{01} - α plane for $Pe_1 = 2$ and initial concentrations $\phi_{02} = 0.01, 0.05$. For these two different starting concentrations, the state diagrams are similar, confirming our expectation that the state is independent of ϕ_{20} . In the parameter range we considered, the small-on-top structure appears when either the size ratio is large or the initial concentration ϕ_{01} is large, which eventually results in a large concentration gradient $\partial\phi_1/\partial z$. Both factors produce a large cross-interaction term, which drives the larger colloids to the bottom. The solid curve in Fig. 3(a) corresponds to Eq. (17) with $C = 1$, which identifies the boundary of the small-on-top structure rather well.

Figure 3(b) shows the results in the ϕ_{01} - Pe_1 plane for the size ratio $\alpha = 3$ and initial concentrations $\phi_{02} = 0.01, 0.05$. Again, the theoretical curve qualitatively explains the

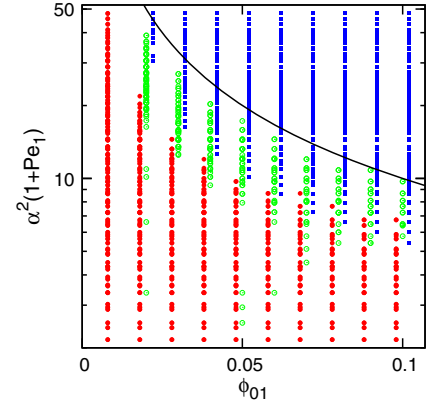


FIG. 4. Master plot of the state diagram in the ϕ_{01} - $\alpha^2(1+Pe_1)$ plane. The solid curve corresponds to $\alpha^2(1+Pe_1)\phi_{01} = 1$. The states labeled by (filled square) and (filled circle) are shifted slightly in the ϕ_{01} axis for a better view.

boundary of the small-on-top region. One should note even at $Pe_1 < 1$, there is noticeable parameter space ($\phi_{01} > 0.05$) where the small-on-top structure appears.

Figure 4 is a master plot collecting all numerical results, where the vertical axis is taken to be $\alpha^2(1+Pe_1)$. The agreement between the theoretical prediction and numerical results is not perfect, but Eq. (17) has captured the general trend of the state boundary.

Discussion and conclusion.—If there is no interaction between colloids, the larger colloids will accumulate near the surface when $Pe_2 > 1$. The condition for this to happen is simply

$$Pe_2 > 1, \quad \text{or} \quad Pe_1 > 1/\alpha. \quad (18)$$

Equation (18) is plotted as the blue line in Fig. 5 for $\alpha = 7$. Above this line, at late times the larger colloids reach close packing earlier than the smaller colloids and form the top layer. However, at early times,

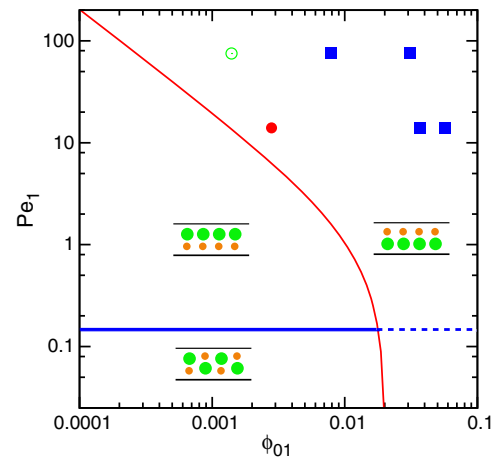


FIG. 5. State diagram when close packing is also considered. The size ratio is $\alpha = 7$. The symbols are results taken from Ref. [13]. The labeling is the same as in Figs. 3 and 4 and discussed in [15].

the concentration gradient of the smaller colloids, combined with a large size asymmetry, results a large cross-interaction term that drives the larger colloids to the bottom. This condition is given by Eq. (17) and is plotted as a red curve in Fig. 5. On the right-hand side of the red curve, the accumulation of larger colloids near the free surface is preempted by the cross interaction at early times.

In Fig. 5, we also compare our results with the simulation and experimental results of Ref. [13], shown in symbols [15]. The overall agreement is good except one experimental data point (the red circle), which also appears to be closest to the transition line.

Extension and improvements can be made in our simple diffusion model. In addition to the binary mixture of colloidal particles, the mixture of polymers and nanoparticles is another interesting system [21,22]. Our theory may shed light on the fabrication of polymer nanocomposite by film drying. The dilute solution limitation can also be removed by using a more general equation of state [23,24]. We have used a simple hard-sphere model, while various types of interaction between colloids can be introduced through the second-order virial coefficient. In our model we also neglect the effect of hydrodynamic interactions. This can be amended by using a concentration-dependent diffusion constant to replace the Stokes value. Nevertheless, we emphasize that the phenomenon described here is quite robust and happens at low concentrations, in the region where our simple diffusion model would be sufficient.

In summary, we have implemented a diffusion model for drying colloidal mixtures that explicitly incorporates the interaction between different colloid types. The smaller colloids exclude the larger colloids and accumulate near the free surface, which stems from the cross interactions. The cross interactions depend on the concentration gradient of the smaller colloids and the large-to-small colloid size ratio. This is a purely out-of-equilibrium phenomenon because the concentration gradient is driven by evaporation. It also happens at low concentrations, in the region where the diffusion model would be sufficient.

This work was supported by the National Natural Science Foundation of China (NSFC) through Grants No. 21434001, No. 21504004, No. 21574006, and No. 21622401. M. D. acknowledges the financial support of the Chinese Central Government via the Thousand Talents Program.

*jjzhou@buaa.edu.cn

*yjiang@buaa.edu.cn

*masao.doi@buaa.edu.cn

- [1] E. Tekin, P. J. Smith, and U. S. Schubert, Inkjet printing as a deposition and patterning tool for polymers and inorganic particles, *Soft Matter* **4**, 703 (2008).
- [2] P. Taylor, The wetting of leaf surfaces, *Curr. Opin. Colloid Interface Sci.* **16**, 326 (2011).
- [3] F. Juillerat, P. Bowen, and H. Hofmann, Formation and drying of colloidal crystals using nanosized silica particles, *Langmuir* **22**, 2249 (2006).
- [4] J. L. Keddie and A. F. Routh, *Fundamentals of Latex Film Formation* (Springer, New York, 2010).
- [5] W. B. Russel, D. A. Saville, and W. R. Schowalter, *Colloidal Dispersions* (Cambridge University Press, Cambridge, England, 1989).
- [6] J. K. G. Dhont, *An Introduction to Dynamics of Colloids* (Elsevier, Amsterdam, 1996).
- [7] M. Doi, *Soft Matter Physics* (Oxford University Press, New York, 2013).
- [8] A. F. Routh, Drying of thin colloidal films, *Rep. Prog. Phys.* **76**, 046603 (2013).
- [9] H. Luo, C. M. Cardinal, L. E. Scriven, and L. F. Francis, Ceramic nanoparticle/monodisperse latex coatings, *Langmuir* **24**, 5552 (2008).
- [10] D. J. Harris, J. C. Conrad, and J. A. Lewis, Evaporative lithographic patterning of binary colloidal films, *Phil. Trans. R. Soc. A* **367**, 5157 (2009).
- [11] R. E. Trueman, E. L. Domingues, S. N. Emmett, M. W. Murray, and A. F. Routh, Auto-stratification in drying colloidal dispersions: A diffusive model, *J. Colloid Interface Sci.* **377**, 207 (2012).
- [12] A. K. Atmuri, S. R. Bhatia, and A. F. Routh, Autostratification in drying colloidal dispersions: Effect of particle interactions, *Langmuir* **28**, 2652 (2012).
- [13] A. Fortini, I. Martín-Fabiani, J. L. De La Haye, P.-Y. Dugas, M. Lansalot, F. D'Agosto, E. Bourgeat-Lami, J. L. Keddie, and R. P. Sear, Dynamic Stratification in Drying Films of Colloidal Mixtures, *Phys. Rev. Lett.* **116**, 118301 (2016).
- [14] A. F. Routh and W. B. Zimmerman, Distribution of particles during solvent evaporation from films, *Chem. Eng. Sci.* **59**, 2961 (2004).
- [15] See Supplemental Material at <http://link.aps.org/supplemental/10.1103/PhysRevLett.118.108002> for the phase diagram, the derivation based on Onsager principle, the dimensionless equations, and the comparison to the results of Ref. [13], which includes Ref. [16].
- [16] S. R. de Groot and P. Mazur, *Non-Equilibrium Thermodynamics* (Dover, New York, 1984).
- [17] R. W. Style and S. S. L. Peppin, Crust formation in drying colloidal suspensions, *Proc. R. Soc. A* **467**, 174 (2011).
- [18] M. Tsige and G. S. Grest, Molecular dynamics study of the evaporation process in polymer films, *Macromolecules* **37**, 4333 (2004).
- [19] T. Okuzono, K. Ozawa, and M. Doi, Simple Model of Skin Formation Caused By Solvent Evaporation in Polymer Solutions, *Phys. Rev. Lett.* **97**, 136103 (2006).
- [20] L. Luo, F. Meng, J. Zhang, and M. Doi, Skin formation in drying a film of soft matter solutions: Application of solute based Lagrangian scheme, *Chin. Phys. B* **25**, 076801 (2016).
- [21] N. Jouault, D. Zhao, and S. K. Kumar, Role of casting solvent on nanoparticle dispersion in polymer nanocomposites, *Macromolecules* **47**, 5246 (2014).
- [22] S. Cheng and G. S. Grest, Dispersing nanoparticles in a polymer film via solvent evaporation, *ACS Macro Lett.* **5**, 694 (2016).
- [23] N. F. Carnahan and K. E. Starling, Equation of state for nonattracting rigid spheres, *J. Chem. Phys.* **51**, 635 (1969).
- [24] H. Hansen-Goos and R. Roth, A new generalization of the Carnahan-Starling equation of state to additive mixtures of hard spheres, *J. Chem. Phys.* **124**, 154506 (2006).